Journal of the Serbian Society for Computational Mechanics / Vol. 1 / No. 1, 2007 / pp. 135-143

Modeling of Cell Mechanical Response by Biphasic Models With Activation

M. Kojic[1], V. Isailovic[2], B. Stojanovic[2], N. Filipovic[2]

[1] Harvard School of Public Health, Harvard University
665 Huntington Ave., Boston, MA 02115, USA
e-mail: mkojic@hsph.harvard.edu
[2] Center for Scientific Research of Serbian Academy of Sciences and Arts and University of Kragujevac
Jovana Cvijica bb, Kragujevac, Serbia

Abstract

A biphasic model of cell is presented in the paper. The model consists of the solid and fluid phases with deformation of solid and fluid flow through pores. Relative motion between the solid and fluid governed by Darcy's law. Activation corresponding to the biochemical processes which transform biochemical energy into the mechanical action is included into the model through the active stresses in the selected fiber directions. The activation evolution is specified by a time function.

Solved examples demonstrate applicability of the proposed cell model.

Key words: cell biphasic mechanical model, activation, FE modeling

1. Introduction

It is observed in experimentally that cells have elastic and viscous response when subjected loading. This response can be modeled by solid continuum with viscoelastic constitutive laws. For a recent review of these models see Mofrad et al. (2006). Cells are very complex structures, with water, charged or ucharged micromoleculs, ions and other molecules, and it is hard to find a phenomenological constitutive relationships which can represent cell behavior under complex mechanical and other actions (as osmotic or electric). Various models have been introduced with the aim to represent the real physical composition of the cell, among which are biphasic, i.e. fluid-solid mixture models.

According to biphasic models, a cell can be considered as a solid-fluid mixture continuum, with cytoplasm as the fluid and cytoskeleton as the solid. In the solid-fluid mixture formulation the viscous response comes from the solid fluid interaction. Furthemore, the viscoelasticity can also be included in the solid phase constitutive law. These models can further be extended to three-phasic (fluid-solid-ion) models to include coupling of mechanical, chemical and electrical events. A review of multiphasic cell models is given by Guilak et al. (2006).

We use here the biphasic model of cell as described in Kojic et al. [1] where cartilage is represented as a solid-fluid mixture. The mixture contains elastic porous solid and fluid which

fills the pores. The additional effects arising due to action of osmotic pressure are neglected in the cell model. But, in order to model biochemical processes within the cell which result into mechanical internal mechanical stresses, we include activation within the continnum model, as in muscle modeling [2]-[6].

A review of various cell mechanical models is presented in Mofrad and Kamm [7].

2. Model formulation

Schematics of the biphasic model is shown in Fig. 1. The field variables at a material point of the continuum are: displacement of solid $\mathbf{u}$, relative fluid velocity with respect to solid (Darcy's velocity) $\mathbf{q}$, and fluid pressure p. The total stress within the solid includes the passive part $\boldsymbol{\sigma}_s$; and active part $\boldsymbol{\sigma}^a$, acting along the skeleton fiber direction $\boldsymbol{\xi}_0$ at a material point. The stress $\boldsymbol{\sigma}_s$ can be determined from the constitutive law (e.g. elastic as for cartilage model). On the other hand, the stress $\boldsymbol{\sigma}^a$ can be expressed in terms of the fiber stretch λ_ξ and the activation level (expressed, for example by an activation function)

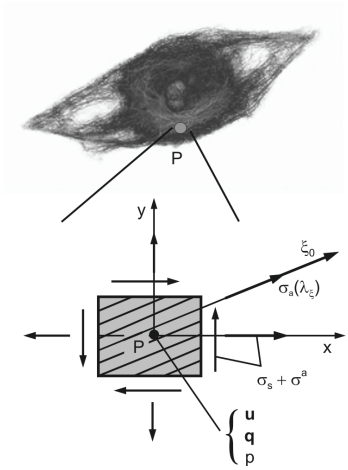

Fig. 1. Biphasic model of cell. Stresses at a material point P within the solid phase include the passive and active parts $\boldsymbol{\sigma}_s$ and $\boldsymbol{\sigma}^a$ (2D representation of stresses in the figure). The stress $\boldsymbol{\sigma}^a$ is acting along the fibers (direction $\boldsymbol{\xi}_0$) and depend on the fiber stretch λ_ξ. The field variables of the model are: displacement of solid $\mathbf{u}$, relative fluid velocity with respect to solid (Darcy's velocity) $\mathbf{q}$, and fluid pressure *p*.

$$\sigma_s^a = \sigma_0 \alpha_a \frac{1-\left(v/v_0\right)}{1+c\left(v/v_0\right)} \tag{1}$$

where σ_0 is the tetanized stress within the fiber, dependent on the fiber stretch λ; $\alpha(t)$ is the time function (activation function) which expresses the muscle activation as a scaling factor for stress with respect to the tetanized state, $0 \le \alpha_a(t) \le 1$ ($\alpha_a = 0$ corresponds to a passive (non-

activated) state, while $\alpha_a = 1$ for a tetanized state); v and v_0 are the velocity and reference velocity of muscle contraction; and c is a material constant.

The governing equations of the model include the balance equations for linear momentum of solid and fluid, and for mass. In the derivations of the equations of balance of linear momentum we have to take into account the interaction force between the solid and fluid arising from the viscous effects described by the Dracy's law. Combining these balance equations for the two phases we finally obtain the equation:

$$\nabla^{\mathrm{T}}\boldsymbol{\sigma} + \rho\mathbf{b} - \rho\ddot{\mathbf{u}} + \rho_f\dot{\mathbf{q}} = \mathbf{0} \tag{2}$$

where b is the body force per unit volume of the mixture; σ is the total stress which can be expressed in terms of σs, $\boldsymbol{\sigma}^a$ and p, as

$$\boldsymbol{\sigma} = (1-n)\left(\boldsymbol{\sigma}_s + \boldsymbol{\sigma}^a\right) - n\mathbf{m}p \tag{3}$$

Here, n is porosity; ρ=(1-n)ρs+nρf is the mixture density, with ρs and ρf being densities of solid and fluid, respectively, and n is porosity; m is a constant vector defined as mT={1 1 1 0 0 0} which provides that the pressure component contributes to the normal stresses only.

Assuming elastic behavior of the solid skeleton, the continuity equation can be written as [8]

$$\nabla^{\mathrm{T}}\mathbf{q} + \left(\mathbf{m}^{\mathrm{T}} - \frac{\mathbf{m}^{\mathrm{T}}\mathbf{C}^{\mathrm{E}}}{3K_s}\right)\dot{\boldsymbol{\varepsilon}} + \left(\frac{1-n}{K_s} + \frac{n}{K_f} - \frac{\mathbf{m}^{\mathrm{T}}\mathbf{C}^{\mathrm{E}}\mathbf{m}}{9K_s^{\,2}}\right)\dot{p} = 0 \tag{4}$$

where $\mathbf{C}^{\mathrm{E}}$ is the elastic constitutive matrix, and K_s and K_f are bulk moduli for the solid skeleton material and fluid, respectively.

The governing equations (2) and (4) can further be transformed into the finite element equations by employing the standard Galerkin method [6], [9-12]. The finite element incremental equations of balance are

$$\begin{bmatrix} \mathbf{M}_{\mathrm{uu}} & \mathbf{0} & \mathbf{0} \\ \mathbf{0} & \mathbf{0} & \mathbf{0} \\ \mathbf{M}_{qu} & \mathbf{0} & \mathbf{0} \end{bmatrix} \begin{Bmatrix} {}^{n+1}\ddot{\mathbf{U}} \\ {}^{n+1}\ddot{\mathbf{P}} \\ {}^{n+1}\ddot{\mathbf{Q}} \end{Bmatrix} + \begin{bmatrix} \mathbf{0} & \mathbf{0} & {}^{n}\mathbf{C}_{\mathbf{uq}} \\ {}^{n}\mathbf{C}_{pu} & \mathbf{C}_{pp} & \mathbf{0} \\ \mathbf{0} & \mathbf{0} & \mathbf{C}_{qq} \end{bmatrix} \begin{Bmatrix} {}^{n+1}\dot{\mathbf{U}} \\ {}^{n+1}\dot{\mathbf{P}} \\ {}^{n+1}\dot{\mathbf{Q}} \end{Bmatrix}$$
$$+ \begin{bmatrix} {}^{n}\mathbf{K}_{\mathbf{uu}} & {}^{n}\mathbf{K}_{\mathbf{u}p} & \mathbf{0} \\ \mathbf{0} & \mathbf{0} & \mathbf{K}_{pq} \\ \mathbf{0} & \mathbf{K}_{qp} & \mathbf{K}_{qq} \end{bmatrix} \begin{Bmatrix} \Delta\mathbf{U} \\ \Delta\mathbf{P} \\ \Delta\mathbf{Q} \end{Bmatrix} = \begin{Bmatrix} {}^{n+1}\mathbf{F}_u \\ {}^{n+1}\mathbf{F}_p \\ {}^{n+1}\mathbf{F}_q \end{Bmatrix} \tag{5}$$

where $\mathbf{U}$, $\mathbf{P}$ and $\mathbf{Q}$ are the nodal vectors for displacement of solid, fluid pressure and Darcy's velocity, respectively; and the left upper indices n and n+1 denote that the quantity is evaluated at the start and end of the current time step n. The matrices and vectors are:

$$\mathbf{M}_{uu}=\int_{{}^{n}\mathbf{V}}\mathbf{N}_u^T\rho\mathbf{N}_u dV,\quad \mathbf{M}_{qu}=\int_{{}^{n}\mathbf{V}}\mathbf{N}_q^T\rho_f\mathbf{N}_u dV,$$

$$\mathbf{C}_{uq}=\mathbf{M}_{qu}^T=\int_{{}^{n}\mathbf{V}}\mathbf{N}_u^T\rho_f\mathbf{N}_q dV,\quad \mathbf{C}_{pu}=-\int_{{}^{n}\mathbf{V}}\mathbf{N}_p^T\left(\mathbf{m}^T-\frac{\mathbf{m}^T\mathbf{C}^E}{3K_s}\right){}^{n}\mathbf{B}dV,$$

$$\mathbf{C}_{pp}=-\int_{{}^{n}\mathbf{V}}\mathbf{N}_p^T\left(\frac{1-n}{K_s}+\frac{n}{K_f}-\frac{\mathbf{m}^T\mathbf{C}^E\mathbf{m}}{9K_s^2}\right)\mathbf{N}_p dV,$$

$$\mathbf{C}_{qq}=\int_{{}^{n}\mathbf{V}}\mathbf{N}_q^T\frac{\rho_f}{n}\mathbf{N}_q dV,$$

$${}^{n}\mathbf{K}_{uu}=\int_{{}^{n}\mathbf{V}}{}^{n}\mathbf{B}^T\mathbf{C}^E{}^{n}\mathbf{B}dV,\quad {}^{n}\mathbf{K}_{up}={}^{n}\mathbf{C}_{pu}^T=\int_{{}^{n}\mathbf{V}}{}^{n}\mathbf{B}^T\left(\frac{\mathbf{C}^E\mathbf{m}}{3K_s}-\mathbf{m}\right)\mathbf{N}_p dV, \tag{6}$$

$$\mathbf{K}_{pq}=\int_{{}^{n}\mathbf{V}}\mathbf{N}_p^T\mathbf{N}_{q,\mathbf{x}}dV,\quad \mathbf{K}_{qp}=\mathbf{K}_{pq}^T=\int_{{}^{n}\mathbf{V}}\mathbf{N}_{q,\mathbf{x}}^T\mathbf{N}_p dV,\quad \mathbf{K}_{qq}=\int_{{}^{n}\mathbf{V}}\mathbf{N}_q^T\mathbf{k}^{-1}\mathbf{N}_q dV,$$

$${}^{n+1}\mathbf{F}_u=\int_{{}^{n}V}\mathbf{N}_u^T\rho^{n+1}\mathbf{b}dV+\int_{{}^{n}A}\mathbf{N}_u^T{}^{n+1}\mathbf{t}dA-\int_{{}^{n}V}{}^{n}\mathbf{B}^T{}^{n}\boldsymbol{\sigma}\,dV-{}^{n}\mathbf{K}_{up}{}^{n}\mathbf{P},$$

$${}^{n+1}\mathbf{F}_p=\int_{{}^{n}A}\mathbf{N}_p^T{}^{n}\mathbf{n}^T{}^{n}\mathbf{q}dA-\mathbf{K}_{pq}{}^{n}\mathbf{Q},$$

$${}^{n+1}\mathbf{F}_q=\int_{{}^{n}V}\mathbf{N}_q^T\rho_f{}^{n+1}\mathbf{b}dV-\mathbf{K}_{qp}{}^{n}\mathbf{P}-\mathbf{K}_{qq}{}^{n}\mathbf{Q}$$

were the quantities are: $\mathbf{N}_u$, $\mathbf{N}_q$ and $\mathbf{N}_p$ are the interpolation matrices for displacements, Darcy's velocities and pressure, respectively; ${}^{n}\mathbf{B}$ is the strain-displacement relation matrix; ${}^{n+1}\mathbf{t}$ is the stress vector on the element surface with the unit normal ${}^{n+1}\mathbf{n}$; and ',x' denotes differentiation with respect to the Cartesian coordinates. These equations can be further written in incremental-iterative form [6]. We note here that the nodal force ${}^{n+1}\mathbf{F}_u$ includes the total stress ${}^{n+1}\boldsymbol{\sigma}$ given in (3), with the activation function at the end of time step.

During iterations we use the density of the mixture ρ, and the porosity n from the start of time step, i.e., ${}^{n}\rho$ and ${}^{n}n$, respectively. After convergence is reached, the porosity is updated by using the continuity equation for fluid, from which the following relation can be obtained [1]:

$${}^{n+1}n={}^{n}n-\Delta t\left[{}^{n}n\,{}^{n}\left(\frac{\partial p}{\partial t}\right)\frac{1}{K_f}+\underline{\nabla}^T{}^{n}\mathbf{q}\right] \tag{7}$$

where Δt is the time step size. In deriving this equation the spatial changes of the fluid density is neglected, i.e. $\partial\rho_f/\partial x_i=0$ is used. This is physically acceptable approximation since the fluid velocity is small, the fluid is nearly incompressible, and the fully saturated conditions are considered.

3. Examples

We present two examples as application of the biphasic model introduced in the previous section.

3.1 Deformation of red blood cell subjected to action optical tweezers

The deformation of red blood cells (RBCs) has been the subject of many investigations. The RBCs deformation is particularly very large during blood flow through capillaries. There, a RBC of a biconcave shape with diameter of around $8\mu m$ passes through capillaries of diameter as small as of $3\mu m$, changing to a bullet shape with large strains, and then recovers its initial shape after leaving the capillaries. This deformability is necessary for mass exchange and normal function of blood. Loss of deformability occurs in severe diseases such as malaria.

Various experimental techniques have been introduced to investigate mechanical characteristics of RBCs, one of which is extension by optical tweezers (Dao et al. [13], Mills et al. [14]). Also, a number of mechanical models have been used for calculating the RBC mechanical response when subjected to loading. One them consist of a shell for the membrane, with neo-Hookean material model, and fluid for cytosol surrounded by the membrane ([13],[14]).

In this example we use elastic material for the membrane and the biphasic model described in Section 2 for the cytosol. Isoparametric 3D finite elements for biphasic medium [6] are used for both the membrane and the cytosol, with the zero-porosity for the membrane. It is assumed that the RBC has initially biconcave shape (Fig. 2a. We model one eight part of the cell (in the first coordinate quadrant) loaded by 1/4F due to symmetry in geometry and loading. The force is distributed on the a part of the surface, as it is in the experiment, and increases slowly so that the quasi-static deformation is assumed. The data used in the model are:

Membrane thickness $\delta = 90\,nm$; Young's moduli for membrane and biphasic model $\left[pN/\mu m^2 \right]$: $1.772\times10^2, 1.5\times10^1$; porosities: n=0. and n=0.7; bulk moduli (for cytosol) $\left[pN/\mu m^2 \right]$: $K_s = 8.3333, K_f = 1.0\cdot10^9$; permeability $k = 1\times10^2\,\mu m^4/pN\,s$.

When the RBC is subjected to axial forces, it deforms into the force action and contracts in the direction normal to the action of forces. The deformed configuration with the displacement field is shown in Fig. 2b. Experimentally recorded and computed shapes (top view) of the deformed cell agree reasonable well (Fig. 2c).

Change of the cell diameters in terms of the extension force F (computed for three values of initial diameters, and experimentally recorded - Dao et al. [13]) in the direction of force action (axial) and in direction orthogonal to this one (transverse in the figure) in terms of the axial force F is shown in Fig. 2d, computed for three initial diameters and measured experimentally. The axial diameter increases and the transverse diameter decreases nonlinearly with the force increase.

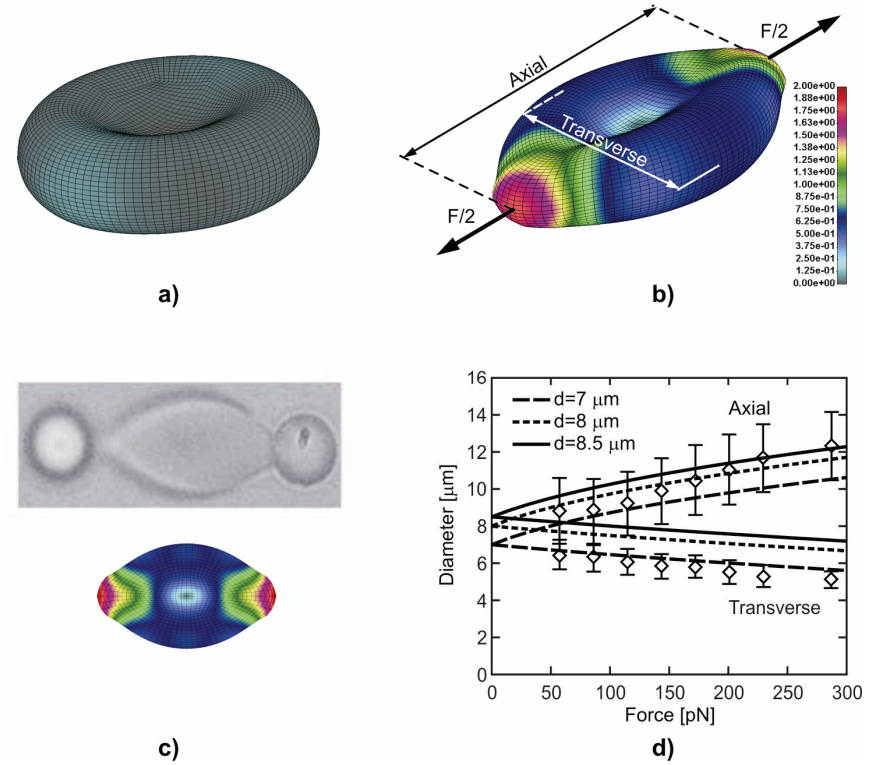

Fig. 2. Biphasic FE model of RBC subjected to uniaxial extension forces. One quarter of the cell is modeled due to symmetry (3D biphasic finite elements). **a)** Initial biconcave shape; **b)** Deformed shape at force of 300 [*pN*]; **c)** Deformed shape (top view) experimentally recorded and computed; **d)** Change of axial and transverse diameters in terms of extensional force for three initial diameters (computed results are represented by lines, and experimental by bars).

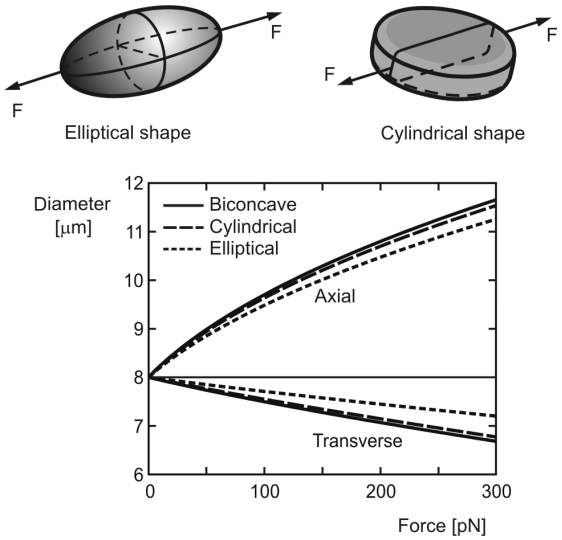

Fig. 3. Computed change of RBC diameters for initial biconcave, cylindrical and elliptical shape. The softest is the biconcave RBC.

We also modeled deformation of RBC assuming cylindrical shape and change of the axial and transverse diameters with the force increase is shown in Fig. 3. It can be seen that, as expected, the RBCs of cylindrical and elliptical shape are stiffer with respect to theRBC of biconcave shape.

The computational results agree reasonably well with experiments and show that the biphasic model can be used for modeling the RBC mechanical response.

3.2 Modeling of cell crawling

In this example we model motion of cell over a plane surface. The cell consists of membrane, interior, nucleus and skeleton. The plane strain 2D model is considered. Initial dimensions, shape and the FE mesh of the cell are shown in Fig. 4b (position 1).

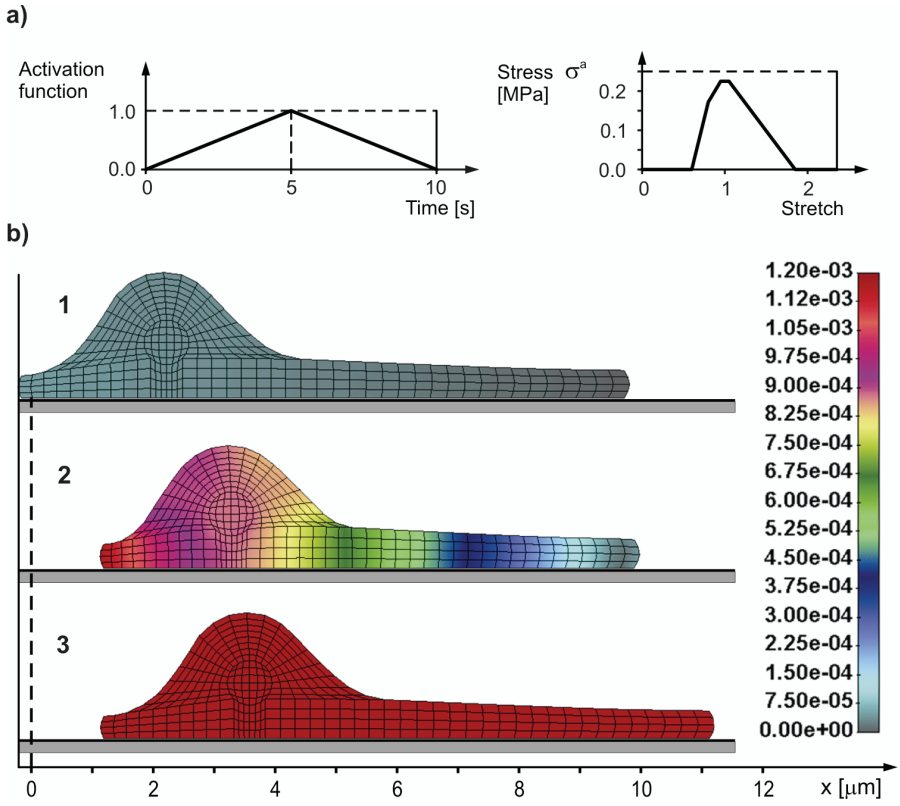

Fig. 4. Crawling of cell over a flat surface (2D plane strain conditions in plane *x-y*). Biphasic model includes: cytoplasm with cytoskeleton and nucleus, and membrane. **a)** Activation function of skeleton structure (left panel) and constitutive law for the active stress $E(z) = E_{HA} + (E_{Ti} - E_{HA})\frac{z}{h}$ (right panel); **b)** Three positions of the cell during crawling (1-initial, after first step; 2-middle, when detachment of the front and attachment of the rear part occur; 3-after relaxation) with the displacement field. Data: Young's moduli [*MPa*] for solid within solid-fluid mixture, and within nucleus $E(r)$ and $E = 0.3$, respectively; initial porosity $n = 0.7$; permeability σ_u^{cor} ; solid and fluid density $\rho(t) = \rho_0 + A(1 - \exp(Bt))$; bulk moduli of solid and fluid $E_{INT} = C\rho^r$, $\sigma_u^{can} = 66\rho^2$.

The membrane and the biphasic medium have the same characteristics as in Example 1. Cytoskeleton is modeled by a set of fibers (truss finite elements) connecting the nodes parallel to the surface and around the nucleus. It is assumed that the nucleus is stiffer than the cell cytoplasm, with no fibers. We use the constitutive law of the fibers shown in Fig. 4a (right panel), with the activation and characteristics of muscle shown in Fig. 4a (left panel). Data are given in the figure caption.

It is assumed that the cell has the protrusion and that it is attached at the front part to the surface (McGrath and Dewey [15]) at the position 1. Then, due to activation the cell deforms and slides over the surface. It is assumed that the activation function is linear (Fig. 4a left panel) reaching maximum at time equal to 5*s*. The deformed cell shape and the displacement field within the cell are shown in the position 2 of the figure. It is then assumed that the cell attaches to the surface at its rear region, with detachment of the protrusion end. Activation decreases to zero and the cell further moves due to relaxation, reaching the initial shape at the position 3.

4. Conclusions

From the presented biphasic model for cell, it can be concluded that the model can be used for representing the mechanical response. Also, by including the activation stress into the model, biochemical processes occurring within the cell can be included and motion of cell caused by the internal 'motors' can be modeled.

Further extension and refinement of this cell model can lead to modeling complex cell biomechanical responses.

The presented examples and others within the cell mechanics and other fields of bioengineering can be solved using the software accompanying the book Kojic M., Filipovic, Stojanovic, Kojic N. [6].

Acknowledgments

This study is partly supported by Ministry of Science and Environmental Protection of Serbia, projects TR6209 and OI144028, and City of Kragujevac.

References

[1] Kojic M, Filipovic N, Mijailovic S (2001). A large strain finite element analysis of cartilage deformation with electrokinetic coupling, Comp. Meth. Appl. Mech. Engrg., 190 , 2447-2464.

[2] Kojic M, Mijailovic S, Zdravkovic N (1998). Modelling of muscle behaviour by the finite element method using Hill's three-element model, *Int. J. Num. Meth. Engrg.*, 43, 941-953.

[3] Stojanovic B (2007). Generalization of Hill's Phenomenological Model in Order to Investigate Muscle Fatigue. Ph.D. Thesis, CIMSI, University of Kragujevac Serbia.

[4] Stojanovic B, Kojic M, Rosic M, Tsui CP, Tang CY (2007). An extension of Hill's three-component model to include different fiber types in finite element modeling of muscle, *Int. J. Num. Meth. Engrg.*, 71, 801-817.

[5] Tang CY, Stojanovic B, Tsui CP, Kojic M (2005). Modeling of muscle fatigue using Hill's model, *Bio-Medical Materials and Engrg.*, 15, 341-348.

[6] Kojic M, Filipovic N, Stojanovic B, Kojic N, Computer Modeling in Bioengineering – Theoretical Background, Examples and Software, J. Wiley and Sons, in press.
[7] Mofrad M R K, Kamm R D: **Cytoskeletal Mechanics**, Cambridge Univ. Press, Cambridge, 2006.
[8] Lewis R.W. and Schrefler B.A., The Finite Element Method in the Deformation and Consolidation of Porous Media, J.Wiley&Sons, Chichester, England, 1987.
[9] Huebner K H, **The Finite Element method for Engineers**, J. Wiley and Sons, New York, 1975.
[10] Hughes T J R, The Finite Element Method. Linear Static and Dynamic Finite Element Analysis, Prentice Hall, Inc., Englewood Cliffs, N.J., 1987.
[11] Kojic M, Slavkovic R, Zivkovic M, Grujovic N, **The Finite Element method – Linear Analysis**, (in Serbian) Faculty of Mech. Eng., Univ. Kragujevac, Serbia, 1998.
[12] Bathe K J, **Finite Element Procedures**, Prentice-Hall, Englewood Cliffs, N. J., 1996.
[13] Dao M, Lim CT, Suresh S, Mechanics of the human red blood cell deformed by optical tweezers, J. Mech. Phys. Solids, 51, 2259-2280, 2003.
[14] Mills JP, Qie L, Dao M, Lim CT, Suresh S, Nonlinear elastic and viscoelastic deformation of the human red blood cell with optical tweezers, MCB, 1(3), 169-180, 2004.
[15] McGrath J L, Dewey C F Jr, Cell dynamics and the actin cytoskeleton, Chapter 9 in: Mofrad M R K, Kamm R D: **Cytoskeletal Mechanics**, Cambridge Univ. Press, Cambridge, 2006.